Range extension for large-scale robotic precision 3D measurements in vibration-prone environments

Daniel Wertjanz, Nikolaus Berlakovich, Ernst Csencsics and Georg Schitter, *Senior member, IEEE*

***Abstract*—This paper presents a range extension concept for a high-precision robotic inline 3D measurement system. A scanning confocal chromatic sensor (SCCS) is integrated with a magnetically levitated and actuated measurement platform for the acquisition of 3D images with sub-micrometer resolution, enabled by means of active sample-tracking to compensate for relative motion between the SCCS and the sample. Based on an intermediate range extension approach, the lateral scan area is pre-extended to enable a robotic repositioning of the 3D measurement module, ensuring sufficient overlap regions between the individual 3D image frames. Experimental results show that the proposed concept extends the 3D measurement modules' measurement range by about 80% of the lateral scan area within an acquisition time of about 90 s. Range-extended 3D measurements directly in a vibration-prone environment reveal that 97% of disturbing relative motion between the SCCS and the sample are compensated by the active sample-tracking approach. In this way, lab-like conditions for the SCCS are established directly in an industrial production line and, improving the measurement error by three orders of magnitude down to several tens of nanometers.**

***Index Terms*—Mechatronics, process control measurements, robotics, acquisition systems.**

I. Introduction

The demand for precision, throughput and quality assurance in the industrial high-tech manufacturing sector is steadily increasing [1]. Flexible and precise inline measurements of industrially produced goods are crucial for enabling the demanded $100\,\%$ quality control [2], [3]. Product quality measurements directly in a production line further allow realtime optimization of production parameter settings, enhancing the overall throughput as well as the production yield [4], [5].

Precise 3D measurements are considered as a key technology, because surface properties, such as topography and roughness, frequently serve as quality indicators in the semiconductor, automotive and consumer electronics sector [6]–[9]. By employing industrial robots, the desired flexible alignment of a 3D measurement tool (MT) at arbitrary measurement locations on a freeform surface [10] as well as the extension of its measurement range [11] can be enabled. However, robots themselves are not suitable for 3D surface measurements with single- or even sub-micrometer resolution [12] as the positioning accuracy of modern industrial robots is in the range of several tens of micrometers [13]. Current robotic 3D measurement systems achieve resolutions down to $50\,\mu\mathrm{m}$ [14], [15].

Manuscript received xxxxxx xx, xxxx; revised xxxxx xx, xxxx.
The authors are with the Automation and Control Institute (ACIN), TU Wien, 1040 Vienna. Corresponding author: wertjanz@acin.tuwien.ac.at

Moreover, environmental vibrations, such as present in an industrial production line, are considered as a major challenge. By causing relative motion between the MT and the sample surface, 3D measurements are corrupted due to motion blur [16]. Therefore, precision 3D measurements are typically conducted in a vibration-free lab environment, making a 100% quality control of goods with structural sizes in the single-micrometer range usually impossible without impairing the throughput.

Active sample-tracking is an appropriate concept for compensating disturbing relative motion between tool and sample, establishing local lab-like conditions during the high-precision 3D measurement [17], [18]. Recently, a robotic inline measurement system for precise 3D surface inspection on freeforms in vibrational environments has been reported [19]. By means of active sample-tracking, the integrated MAGLEV measurement platform (MP) maintains a constant position between the embedded compact and lightweight scanning confocal chromatic sensor (SCCS) [20] and the sample surface. In this configuration, the lateral measurement range of the SCCS ($350 \times 250\,\mu\mathrm{m}^2$) represents a limitation for applications requiring 3D measurements of samples with larger lateral dimensions, such as microlens arrays [21] or stacked IC devices [22]. Using the robot for repositioning the SCCS and acquiring multiple overlapping 3D images [23], which are combined by image registration techniques [24], [25], appears as a viable approach. As the lateral measurement range of the SCCS is comparably small in relation to the positioning uncertainty of the robot, a purely robotic repositioning may cause insufficient overlap region between adjacent 3D measurements and a decreased registration performance.

The contribution of this paper is the integration of a two-step position control approach for repositioning a robot, in order to significantly extend the system's measurement range for operation in a vibration-prone environment.

This paper in an extension of our previous work, which focused mainly on an intermediate range extension concept [26], in which the scan area is enlarged to $500 \times 500\,\mu\mathrm{m}^2$ by using the MP to reposition the SCCS. However, this concept limits the system operation to a static robot position, which may be insufficient for samples with larger lateral dimensions. To further extend the system's lateral measurement range, a robotic repositioning approach is combined with a subsequent registering of several intermediate range-extended 3D measurements acquired in adjacent robot positions, described in detail in Section III. In Section IV, the system performance is evaluated in a vibration-prone environment, while Section V

Post-print version of the article: D. Wertjanz, N. Berlakovich, E. Csencsics, and G. Schitter, "Range extension for large-scale robotic precision 3D measurements in vibration-prone environments," *IEEE Transactions on Instrumentation and Measurement*,Early Access Version, 2022. DOI: 10.1109/TIM.2023.3268473

concludes the paper.

II. Measurement Module for Robotic Applications

The system concept for precise robot-based inline 3D measurements on freeform surfaces within vibration-prone environments is illustrated in Fig.1. Acting as a robot end-effector, the measurement module comprises a SCCS as high-precision 3D MT mounted on a MAGLEV MP, with tracking sensors measuring the position of the SCCS relative to the sample surface to be inspected. Independent on the actual robot pose, a constant alignment of the MT to the sample surface is maintained by means of an integrated feedback control. The resulting contactless stiff link between SCCS and sample surface actively compensates for relative motion and establishes lab-like conditions for the 3D MT directly in vibrational environments.

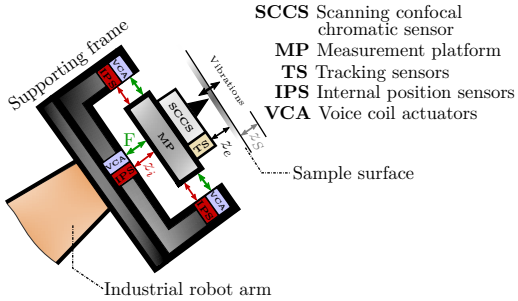

(a) Measurement module for robotic applications.

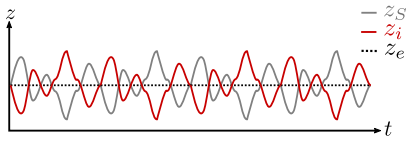

(b) Position signals.

Fig. 1: System concept of robotic inline precision 3D measurements on freeform surfaces. a) By maintaining a constant alignment z_e between the SCCS and the sample surface, disturbing vibrations z_S are actively compensated. b) In the internal position signal z_i, the tracking motion is visible, compensating the sample vibrations z_S.

Considering the concept in Fig. 1, Fig. 2 shows the implemented measurement system prototype with an active sample-tracking MP [19]. An industrial robot arm (KR 10 R900-2, KUKA AG, Augsburg, Germany) is used to coarsely align the measurement system to an arbitrary location on a sample surface. With consideration of the targeted large-scale precision 3D measurements, a precise repositioning of the industrial robot to adjacent measurement locations is required. However, as the lateral measurement range of the SCCS ($350 \times 250\,\mu m^2$) is comparably small in relation to the positioning uncertainty of the robot, it may cause insufficient overlap regions between the individual image frames. Therefore, an intermediate range extension concept using the MP for repositioning has been proposed, enlarging the measurement range to about $500 \times 500\,\mu m^2$ in a static robot position [26].

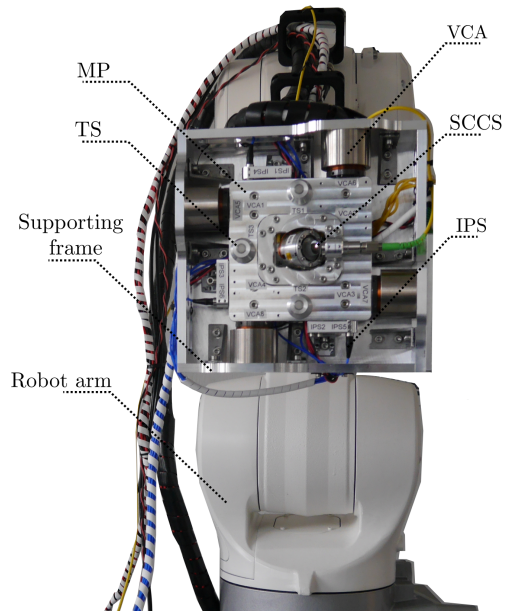

Fig. 2: Robotic inline measurement system for precise 3D surface inspection in vibrational environments. The vibration-compensating measurement module, with the SCCS as 3D MT on the MP, is mounted on an industrial robot arm.

A. Scanning confocal chromatic sensor

In order to achieve the targeted precision 3D measurements, the lightweight SCCS in Fig. 3 has been developed as a 3D MT [20]. Having a compact size of $75 \times 63 \times 55\,mm^3$, the SCCS is tailored for integration onto the MAGLEV MP. By manipulating the optical path of a high precision 1D confocal chromatic sensor (CCS) with a high performance fast steering mirror (FSM) [27], the measuring light spot is scanned across the sample surface to be inspected. A multi-input-multi-output (MIMO) H_∞ controller is implemented to achieve high performance motion control of the two FSM axes. An efficient and dense scanning motion is achieved by applying Lissajous trajectories to the FSM axes. Using a data-driven image reconstruction procedure, the FSM deflection angles and the correspondingly measured distances are combined to obtain an accurate 3D surface measurement. The measurement volume of about $350 \times 250 \times 1800\,\mu m^3$ can be imaged with frame rates of up to 1 fps. High resolution scans can be performed with a lateral and axial resolution of down to $2.5\,\mu m$ and 76 nm, respectively. A detailed discussion on the SCCS' system design as well as an experimental validation of the achieved performance can be found in [20].

B. Module for active sample-tracking

Being a core component of the entire measurement system, the integrated tracking module comprises a MAGLEV

Post-print version of the article: D. Wertjanz, N. Berlakovich, E. Csencsics, and G. Schitter, "Range extension for large-scale robotic precision 3D measurements in vibration-prone environments," *IEEE Transactions on Instrumentation and Measurement*,Early Access Version, 2022. DOI: 10.1109/TIM.2023.3268473

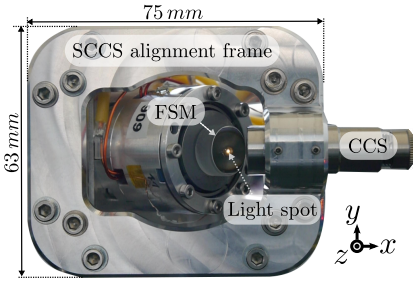

Fig. 3: Compact SCCS for precision 3D measurements. Using a high performance FSM, the light spot of the CCS is precisely scanned across the sample surface for acquiring the topography.

MP [19]. Eight identical voice coil actuators (VCAs) are placed around the MP, yielding a balanced system design and enabling operation in arbitrary orientations [28]. The MP is freely floating and actuated within the air gaps of the VCAs. As internal position sensor (IPS) system, six capacitive displacement sensors (CSH05, Micro-Epsilon, Ortenburg, Germany) are used to measure the MP's position relative to the supporting frame. Each sensor shows a measurement range of $500\,\mu\mathrm{m}$ with a constant gain of $50\,\mu\mathrm{m\,V^{-1}}$.

The measured internal position is used in feedback control to maintain a free-floating position with respect to the supporting frame (stabilization mode) when repositioning the robot. Additionally, three capacitive tracking sensors (TSs) of the same type as the IPSs are included, measuring the MP's out-of-plane position relative to a sample surface. Thus, the system is capable of actively tracking a sample surface in the out-of-plane degrees of freedom (DoFs), while being stabilized in-plane. As a high tracking performance of the MP is desired, $600\,\mathrm{Hz}$ proportional-integral-derivative (PID) position controllers are designed and implemented to individually control each DoF. The MP can be positioned with a positioning uncertainty of $17\,\mathrm{nm\,rms}$ either to its supporting frame or a sample surface.

III. Range Extension Concept

The SCCS' lateral measurement range ($350 \times 250\,\mu\mathrm{m}^2$) is limited by the maximum deflection of the FSM and the axial measurement range of the CCS [20], which may not be sufficient for some sample surfaces. To ensure a robust 3D image registration when moving the robot arm to enlarge the SCCS' lateral measurement range, the scan area is desired to be a factor of 10 higher than the positioning uncertainty of an industrial robot, being typically about $50\,\mu\mathrm{m}$ [13]. In a first step towards the targeted precision 3D measurements on a larger scale and to ensure sufficient overlap regions between adjacent 3D image frames before repositioning the robot, an intermediate range extension of the SCCS' lateral scan area has been developed [26]. With the enlarged lateral measurement range in a static robot position to a scan area of $500 \times 500\,\mu\mathrm{m}^2$, non-overlap regions are avoided when repositioning the robot to the next measurement spot. The novel integrated approach in Fig. 4 includes the previously proposed intermediate range extension concept, which is broadened by a robot repositioning to enable the targeted large-scale robotic precision 3D measurements.

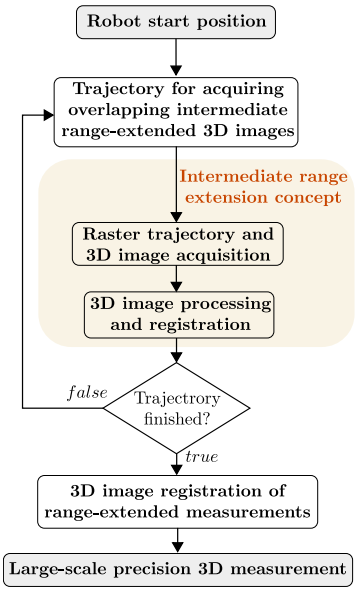

Fig. 4: Concept for robotic precision 3D measurements on larger scale surfaces. An in advance planned measurement trajectory is performed by the robot. After each robotic repositioning, the intermediate range extension procedure from [26] is applied. As a result of the subsequent 3D image registration algorithm, the targeted large-scale precision 3D measurement is obtained.

A. Intermediate range extension

By using the MP to position the SCCS at multiple measurement spots, fast and precise repositioning is enabled, yielding an efficient intermediate range extension (see yellow area in Fig. 4). In order to achieve a smooth and efficient repositioning of the SCCS between the 3×3 measurement locations, minimum jerk trajectories are applied to the MP's in-plane position control. At each measurement location, a full-range 3D image is acquired, resulting in nine individual 3D images with a defined overlap region between the adjacent frames. During a measurement, a constant alignment of the SCCS relative to the sample surface is desired. Therefore, the MP operates in tracking mode, i.e it actively tracks the sample surface in the three out-of-plane DoFs z, ϕ_x and ϕ_y.

As position uncertainties may occur when merging the individual 3D images using their nominal positions, a parallel registration algorithm [25] is applied for stitching the individual 3D measurements together. This algorithm reduces the resulting overlap mismatch between the 3D images, yielding precise and fast registration of the individual 3D measurements. The registration is performed in an iterative manner and takes about $300\,\mathrm{ms}$ on a personal computer. Experimental

Post-print version of the article: D. Wertjanz, N. Berlakovich, E. Csencsics, and G. Schitter, "Range extension for large-scale robotic precision 3D measurements in vibration-prone environments," *IEEE Transactions on Instrumentation and Measurement*,Early Access Version, 2022. DOI: 10.1109/TIM.2023.3268473

results demonstrate an extension of the SCCS' scan area by a factor of 3 to $500 \times 500\,\mu\text{m}^2$, while achieving a measurement error of only $60\,\text{nm}$ in the entire range-extended 3D measurement and demonstrating the ability to successfully measure surface defects. A detailed description of the intermediate range extension concept can be found in [26].

B. Range-extended robotic precision 3D measurement concept

Based on the intermediate range extension concept to avoid insufficient overlap regions, a robotic repositioning procedure is developed to further extend the 3D measurement system's lateral scan area. The robot trajectory indicated in the flow chart in Fig. 4 is planned in advance and can be adapted to the lateral dimension of the sample under test. Depending on the shape, complexity and surface of the sample under test, overlap regions of varying size may be required for a robust 3D image registration. To achieve overlap regions between 10% and 90% of the intermediate range-extended measurement area ($500 \times 500\,\mu\text{m}^2$), the robot trajectory can therefore be adapted via a variable lateral repositioning between $50\,\mu\text{m}$ and $450\,\mu\text{m}$ relative to the sample. Considering for example an overlap region of 20%, equalling robotic repositioning steps of about $400\,\mu\text{m}$, three adjacent robot positions are necessary to extend the system's measurement range to the single-millimeter scale. In each robot position, an intermediate range-extended 3D image is acquired and stored together with the robot position measured by the robot's internal encoders.

Similar to the MP-based SCCS repositioning [26], using only the robot position to register the sub-measurements would cause a residual uncertainty of the individual intermediate range extended measurements in the global image frame. Therefore, a registration and 3D image processing procedure is applied subsequently to the intermediate range-extended 3D image acquisition with the robotic measurement trajectory being finished. The used registration algorithm [29] minimizes the metric

$$\mathfrak{M}_g(\boldsymbol{A}) = \sum_{i,k} \mathfrak{M}_{ik}(\mathbf{a}_i, \mathbf{a}_k) \tag{1}$$

for the entire overlap mismatch between the intermediate range-extended measurements in a parallel registration manner. In this relation, $\mathfrak{M}_{ik}(\mathbf{a}_i, \mathbf{a}_k)$ denotes the metric for the overlap mismatch between segment i and k, which are transformed by the registering parameters $\mathbf{a}_i \in \mathbb{R}^6$ and $\mathbf{a}_k \in \mathbb{R}^6$, respectively. The registering parameters for an intermediate range-extended measurement are a set of 6 parameters, which define a rigid-body transformation. In addition to the minimization of Eq. 1, the algorithm incorporates a priori information about the registering parameters, which further improves the registration performance [29].

IV. Experimental Evaluation of the Range-Extended 3D Imaging Performance

The proposed concept for extending the 3D imaging range of the SCCS from Section III is experimentally validated using a silicon step height standard (Nanuler Calibration Standard, Applied NanoStructures Inc., Mountain view, CA, USA) with a nominal structural height of $5.81\,\mu\text{m}$. In Fig. 5, a microscope image of the first two letters of the manufacturer's logo is shown, which is selected as test structure. As can be clearly seen, a surface defect is located on the bottom-right of the first letter "N", which may be a scratch.

Considering the concept discussed in Section III, the dashed red ($\mathbf{IM_1}$) and green area ($\mathbf{IM_2}$) indicate the two intermediate range-extended 3D measurement areas at two adjacent robotic measurement locations. In this relation, the robot trajectory consists of a single 3D measurement module repositioning step, which, however, can be simply adapted to different samples. Note that the shape of each intermediate range-extended 3D measurement is caused by the MP-based SCCS positioning at 3×3 measurement spots and the rhomboidal shape of its lateral measurement area. Each individual 3D measurement is performed by applying driving frequencies of $5.7\,\text{Hz}$ and $4.3\,\text{Hz}$ to the tip and tilt axis of the FSM, yielding a dense Lissajous scan pattern, high lateral resolution and a measurement time of $T = 10\,\text{s}$ [20]. For the sample surface shown in Fig. 5, an overlap region of about 20% is selected, which is sufficient for a robust 3D image registration of $\mathbf{IM_1}$ and $\mathbf{IM_2}$.

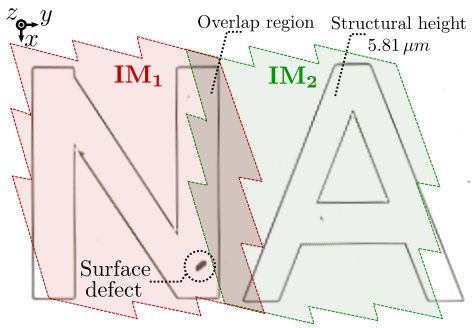

Fig. 5: Microscope image of the test structure with the two measurement locations $\mathbf{IM_1}$ and $\mathbf{IM_2}$. The sample comprises the letters "NA" with a structural height of $5.81\,\mu\text{m}$ and a surface defect. An overlap region of about 20% is indicated by the dark area.

A. Intermediate range extension in vibrational environment

In a first step, the system performance of the intermediate range extension concept [26] is evaluated in a vibrational environment. To emulate the desired industrial-like environment, a 1-DoF shaker is used as disturbance generator [19]. According to the vibration criteria presented in [30], environmental vibrations have significant components in the frequency range between 4 and $80\,\text{Hz}$. In this relation, the sample is mounted on the 1-DoF shaker, to which a randomized signal according to the VC-A norm [30] is applied, resulting in a $7.8\,\mu\text{m}\,\text{rms}$ disturbance motion in DoF z.

Using the industrial robot, the 3D measurement module is aligned to the sample surface on the shaker. The time signal of the relative motion between the SCCS and the sample surface is represented by the positioning error e of DoF z in red in Fig. 6 for disabled sample-tracking. Repeating the measurement with active sample-tracking, a residual error

Post-print version of the article: D. Wertjanz, N. Berlakovich, E. Csencsics, and G. Schitter, "Range extension for large-scale robotic precision 3D measurements in vibration-prone environments," *IEEE Transactions on Instrumentation and Measurement*,Early Access Version, 2022. DOI: 10.1109/TIM.2023.3268473

of only 228 nm rms is obtained (black). Thus, the feedback control-induced stiff link between the SCCS and the sample surface is capable of attenuating 97 % of the vibration-induced relative motion in DoF z.

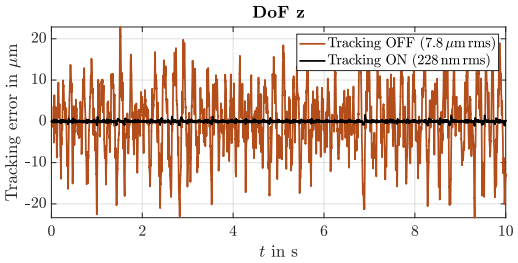

Fig. 6: Active sample-tracking performance in DoF z. The relative motion of 7.8 µm rms induced by the shaker is indicated in red (disabled tracking control). By enabling the tracking control (black), a residual error of 228 nm rms is achieved.

Using the proposed MP-based intermediate range extension concept [26], a reference measurement of the letter "A" ($\mathbf{IM_2}$ in Fig. 5) is performed in static lab conditions with the shaker turned off and the 3D measurement module in tracking mode. The results related to this experiment are shown in Fig. 7a. The acquisition time of the 3×3 individual 3D images is about $9T = 90\,\mathrm{s}$ as the time for the fast MP repositioning (50 ms) is neglectable. Sufficient overlap regions between the 3×3 individual 3D image frames are ensured, resulting in a robust image registration, performed in only 300 ms on a personal computer. By turning off the sample-tracking and applying the vibrations to the sample, motion blur appears in the intermediate range-extended 3D measurement (Fig. 7b), making the sample's surface structure hardly visible and impeding a robust 3D image registration. Repeating the measurement with active sample-tracking, the relative motion between SCCS and sample is compensated and surface structure of in the targeted scan area $\mathbf{IM_2}$ in Fig. 7c is clearly visible.

Next, the dashed red cross sections at $x = 250\,\mu\mathrm{m}$ in Fig. 7a - 7c are analyzed in Fig. 7d. In case of disabled tracking control, the vibration-induced relative motion causes an incorrectly measured sample height of 15.4 µm (red), equivalent to a measurement error of 9.59 µm. For enabled sample-tracking (solid black), the obtained cross section is similar to the one in the reference measurement (dashed black). A structural height of 5.82 µm is measured, equalling a measurement error of only 10 nm is achieved (see Fig. 5). Compared to the incorrectly measured structural height with disabled tracking control, the intermediate range-extended 3D measurement uncertainty is reduced by a factor of $\frac{9.59\,\mu\mathrm{m}}{10\,\mathrm{nm}} = 959$.

B. Range-extended robotic precision 3D measurements

Finally, the robotic range extension concept in Fig. 4 is evaluated under lab conditions and in a vibration-prone environment. With consideration of the chosen sample in Fig. 5, two individual intermediate range extended 3D measurements $\mathbf{IM_1}$ and $\mathbf{IM_2}$ are required. Therefore, the 3D measurement system is positioned in its initial robotic position ($\mathbf{RP_1}$) and an intermediate range-extended measurement of the scan area $\mathbf{IM_1}$ is performed. Next, the robot is repositioned with respect to the sample ($\mathbf{RP_2}$) by applying a position step of 400 µm in the lateral DoF x, resulting in an overlap region of about 20% of the intermediate range extended lateral scan area ($500 \times 500\,\mu\mathrm{m}^2$). After performing the intermediate range-extended 3D image of the second scan area $\mathbf{IM_2}$, the robot trajectory is finished (see Fig. 4) and the tailored 3D image registration algorithm [29] is applied. The entire acquisition time of this range-extended measurement is about $2 \cdot 90\,\mathrm{s}$, which is the time for acquiring $\mathbf{IM_1}$ and $\mathbf{IM_2}$, as the image processing and registration time is about two orders of magnitude smaller and therefore neglectable. Thus, a robotic measurement range extension by about 80% of the lateral scan area ($500 \times 500\,\mu\mathrm{m}^2$) is performed within 90 s.

In Fig. 8a, the range-extended 3D measurement under lab conditions is shown. As can be seen, the robotic 3D measurement module's lateral measurement range is successfully extended to the targeted scan area indicated in Fig. 5, with the surface defect on the bottom-right of the letter "N" clearly visible. Repeating the robotic measurement procedure with disturbances applied to sample and enabled tracking control, the 3D image in Fig. 8b results. Again, the defect is visible, highlighting the system's capability to detect surface defects within a vibration-prone environment. By analyzing the red cross section of Fig. 8a and 8b in Fig. 8c, a similar result can be seen with a measured structural height of 5.78 µm, equalling a measurement error of 30 nm.

In summary, the proposed concept successfully enlarges the robotic 3D measurement system's lateral measurement range, while the active sample-tracking MP establishes lab-like conditions for the SCCS by compensating 97% of disturbing vibrations, which improves the 3D measurement error by three orders of magnitude down to several tens of nanometers.

V. Conclusion

In this paper, a range extension concept for a precise robotic inline 3D measurement system is presented. The 3D MT is mounted to a MAGLEV MP, which is capable of actively tracking a sample surface in the out-of-plane DoFs. As the SCCS' lateral scan area is relatively small compared to the position uncertainty of an industrial robot, a purely robot-based measurement range extension may cause insufficient overlap regions between the individual 3D measurements. Therefore, the MP is used to precisely position the 3D MT at multiple measurement locations, enabling an efficient intermediate range extension of the SCCS' lateral scan area. In this way, the lateral scan area is sufficiently enlarged to enable a robotic repositioning of the 3D measurement module, avoiding insufficient overlap regions between adjacent intermediate range-extended 3D measurements. The proposed concept extends the 3D measurement modules' measurement range by about 80% of the lateral scan area ($500 \times 500\,\mu\mathrm{m}^2$) within a time of about 90 s. Experimental results in a vibration-prone environment show that 97% of disturbing relative motion between the SCCS and the sample are compensated by the active sample-tracking control, establishing the desired lab-like conditions for the

Post-print version of the article: D. Wertjanz, N. Berlakovich, E. Csencsics, and G. Schitter, "Range extension for large-scale robotic precision 3D measurements in vibration-prone environments," *IEEE Transactions on Instrumentation and Measurement*,Early Access Version, 2022. DOI: 10.1109/TIM.2023.3268473

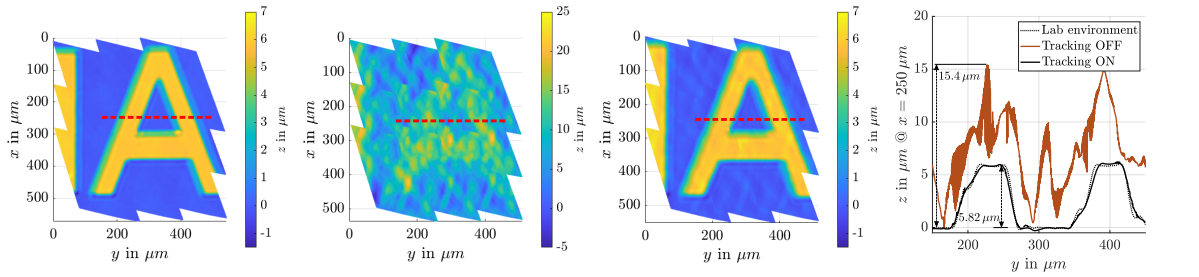

(a) Lab environment. (b) Tracking off. (c) Tracking on. (d) Cross section at $x = 250\,\mu\text{m}$.

Fig. 7: Intermediate range-extended precision 3D measurement of $\mathbf{IM_2}$ (see Fig. 5). a) shows the reference 3D measurement under lab conditions. With disabled tracking control in b), the vibration-induced relative motion causes motion blur in the 3D measurement. In c), the intermediate range-extended 3D measurement result for enabled sample-tracking is shown. The surface structure is clearly visible. In d), the cross sections (dashed red) at $x = 250\,\mu\text{m}$ of a)-c) are analyzed. For disabled tracking control, the applied vibrations cause an incorrect sample height of $15.4\,\mu\text{m}$ (red). By enabling the active sample-tracking (solid black), a similar cross section as for the reference measurement (dashed black) is obtained with a measured sample height of $5.82\,\mu\text{m}$.

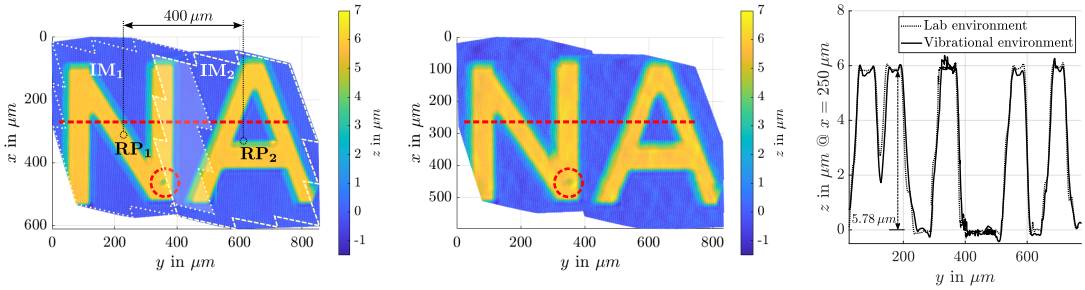

(a) Lab conditions. (b) Vibration-prone environment. (c) Cross section at $x = 250\,\mu\text{m}$.

Fig. 8: Precise robotic range-extended 3D measurements. In a), a reference measurement of the sample with the targeted scan area indicated in Fig. 5 is shown. $\mathbf{RP_1}$ and $\mathbf{RP_2}$ indicate the two robotic positions in which the two intermediate range-extended measurements $\mathbf{IM_1}$ and $\mathbf{IM_2}$ are performed. The surface defect on the bottom-right of the letter "N" is clearly visible. The range-extended 3D measurement with active sample-tracking in a vibration-prone environment is shown in b), with the surface defect again being visible. c) compares the cross sections of a) and b) indicated in dashed red. A very similar structure and a height of $5.78\,\mu\text{m}$ is measured in both the lab and vibrational environment.

SCCS. Comparing the range-extended 3D measurement performance achieved by active sample-tracking with the motion blur-corrupted result obtained with disabled tracking control, the measurement uncertainty is reduced by three orders of magnitude. Moreover, while achieving a measurement error of only several tens of nanometers in the entire range-extended 3D measurement, the system's ability to detect surface defects under vibration-prone conditions is demonstrated.

ACKNOWLEDGMENTS

This project is partially funded by the Hochschuljubilaeumsfonds of the city of Vienna, Austria under the project number H-260744/2020. The financial support by the Austrian Federal Ministry for Digital and Economic Affairs, and the National Foundation for Research, Technology and Development, as well as MICRO-EPSILON MESSTECHNIK GmbH & Co. KG and ATENSOR Engineering and Technology Systems GmbH is gratefully acknowledged.

REFERENCES

[1] T. Uhrmann, T. Matthias, M. Wimplinger, J. Burggraf, D. Burgstaller, H. Wiesbauer, and P. Lindner, "Recent progress in thin wafer processing," in *2013 IEEE International 3D Systems Integration Conference (3DIC)*, 2013, pp. 1–8.

[2] D. Imkamp, R. Schmitt, and J. Berthold, "Blick in die Zukunft der Fertigungsmesstechnik - Die VDI/VDE-GMA Roadmap Fertigungsmesstechnik 2020." *Technisches Messen*, vol. 10, no. 79, 2012.

[3] R. Schmitt and F. Moenning, "Ensure success with inline-metrology," in *XVIII IMEKO World Congress - Metrology for a Sustainable Development*, 2006.

[4] W. Gao, H. Haitjema, F. Fang, R. Leach, C. Cheung, E. Savio, and J. Linares, "On-machine and in-process surface metrology for precision manufacturing," *CIRP Annals*, vol. 68, no. 2, pp. 843 – 866, 2019.

[5] M. Grasso and B. Colosimo, "Process defects and in situ monitoring methods in metal powder bed fusion: a review," *Measurement Science and Technology*, vol. 28, p. 044005, 2017.

Post-print version of the article: D. Wertjanz, N. Berlakovich, E. Csencsics, and G. Schitter, "Range extension for large-scale robotic precision 3D measurements in vibration-prone environments," *IEEE Transactions on Instrumentation and Measurement*,Early Access Version, 2022. DOI: 10.1109/TIM.2023.3268473

[6] A. Yogeswaran and P. Payeur, "3d surface analysis for automated detection of deformations on automotive body panels," in *New Advances in Vehicular Technology and Automotive Engineering*. IntechOpen, 2012.
[7] T.-F. Yao, A. Duenner, and M. Cullinan, "In-line dimensional metrology in nanomanufacturing systems enabled by a passive semiconductor wafer alignment mechanism," *Journal of Micro- and Nano-Manufacturing*, vol. 5, no. 1, 2016.
[8] G. Sansoni, M. Trebeschi, and F. Docchio, "State-of-the-art and applications of 3d imaging sensors in industry, cultural heritage, medicine, and criminal investigation," *Sensors (Basel, Switzerland)*, vol. 9, pp. 568–601, 2009.
[9] H. Schwenke, U. Neuschaefer-Rube, T. Pfeifer, and H. Kunzmann, "Optical methods for dimensional metrology in production engineering," *CIRP Annals*, vol. 51, no. 2, pp. 685–699, 2002.
[10] E. Savio, L. D. Chiffre, and R. Schmitt, "Metrology of freeform shaped parts," *CIRP Annals*, vol. 56, no. 2, pp. 810 – 835, 2007.
[11] J. Rejc, J. Cinkelj, and M. Munih, "Dimensional measurements of a gray-iron object using a robot and a laser displacement sensor," *Robotics and Computer-Integrated Manufacturing*, vol. 25, no. 2, pp. 155–167, 2009.
[12] E. Csencsics, M. Thier, S. Ito, and G. Schitter, "Supplemental peak filters for advanced disturbance rejection on a high precision endeffector for robot-based inline metrology," *IEEE/ASME Transactions on Mechatronics (Early Access)*, pp. 1–1, 2021.
[13] U. Schneider, M. Drust, M. Ansaloni, C. Lehmann, M. Pellicciari, F. Leali, J. Gunnink, and A. Verl, "Improving robotic machining accuracy through experimental error investigation and modular compensation," *The International Journal of Advanced Manufacturing Technology*, vol. 85, pp. 1–13, 2014.
[14] S. Yin, Y. Ren, Y. Guo, J. Zhu, S. Yang, and S. Ye, "Development and calibration of an integrated 3d scanning system for high-accuracy large-scale metrology," *Measurement*, vol. 54, pp. 65–76, 2014.
[15] G. B. de Sousa, A. Olabi, J. Palos, and O. Gibaru, "3d metrology using a collaborative robot with a laser triangulation sensor," *Procedia Manufacturing*, vol. 11, pp. 132–140, 2017.
[16] R. Saathof, M. Thier, R. Hainisch, and G. Schitter, "Integrated system and control design of a one dof nano-metrology platform," *Mechatronics*, vol. 47, pp. 88 – 96, 2017.
[17] S. Ito, B. Lindner, and G. Schitter, "Sample-tracking vibration isolation with hybrid reluctance actuators for inline metrology," in *Proceedings of the Joint Conference 8th IFAC Symposium on Mechatronic Systems (MECHATRONICS 2019), and 11th IFAC Symposium on Nonlinear Control Systems (NOLCOS 2019)*, vol. 52/15, 2019.
[18] M. Thier, R. Saathof, A. Sinn, R. Hainisch, and G. Schitter, "Six degree of freedom vibration isolation platform for in-line nano-metrology," *IFAC-PapersOnLine*, vol. 49, no. 21, pp. 149–156, 2016, 7th IFAC Symposium on Mechatronic Systems MECHATRONICS 2016.
[19] D. Wertjanz, T. Kern, E. Csencsics, and G. Schitter, "Bringing the lab to the fab: Robot-based inline measurement system for precise 3d surface inspection in vibrational environments," *IEEE Transactions on Industrial Electronics*, 2021, submitted.
[20] D. Wertjanz, T. Kern, E. Csencsics, G. Stadler, and G. Schitter, "Compact scanning confocal chromatic sensor enabling precision 3-d measurements," *Appl. Opt.*, vol. 60, no. 25, pp. 7511–7517, 2021.
[21] A. Peer, R. Biswas, J.-M. Park, R. Shinar, and J. Shinar, "Light management in perovskite solar cells and organic leds with microlens arrays," *Optics express*, vol. 25, no. 9, pp. 10 704–10 709, 2017.
[22] M. Liebens, A. Jourdain, J. De Vos, T. Vandeweyer, A. Miller, E. Beyne, S. Li, G. Bast, M. Stoerring, S. Hiebert, and A. Cross, "In-line metrology for characterization and control of extreme wafer thinning of bonded wafers," *IEEE Transactions on Semiconductor Manufacturing*, vol. 32, no. 1, pp. 54–61, 2019.
[23] A. Paoli and A. V. Razionale, "Large yacht hull measurement by integrating optical scanning with mechanical tracking-based methodologies," *Robotics and Computer-Integrated Manufacturing*, vol. 28, no. 5, pp. 592–601, 2012.
[24] P. J. Besl and N. D. McKay, "Method for registration of 3-d shapes," in *Sensor fusion IV: control paradigms and data structures*, vol. 1611. International Society for Optics and Photonics, 1992, pp. 586–606.
[25] N. Berlakovich, E. Csencsics, M. Fuerst, and G. Schitter, "Iterative parallel registration of strongly misaligned wavefront segments," *Opt. Express*, vol. 29, no. 21, pp. 33 281–33 296, 2021.
[26] D. Wertjanz, N. Berlakovich, E. Csencsics, and G. Schitter, "Range extension of a scanning confocal chromatic sensor for precise robotic inline 3d measurements," in *2022 IEEE International Instrumentation and Measurement Technology Conference (I2MTC)*, 2022, pp. 1–6.
[27] E. Csencsics, J. Schlarp, T. Schopf, and G. Schitter, "Compact high performance hybrid reluctance actuated fast steering mirror system," *Mechatronics*, vol. 62, p. 102251, 2019.
[28] D. Wertjanz, E. Csencsics, J. Schlarp, and G. Schitter, "Design and control of a maglev platform for positioning in arbitrary orientations," in *2020 IEEE/ASME International Conference on Advanced Intelligent Mechatronics (AIM)*, 2020, pp. 1935–1942.
[29] N. Berlakovich, M. Fuerst, E. Csencsics, and G. Schitter, "Improving the precision of parallel registration by incorporating a priori information," *Opt. Express*, 2022, in review.
[30] C. G. Gordon, "Generic vibration criteria for vibration-sensitive equipment," in *Optomechanical Engineering and Vibration Control*, vol. 3786, International Society for Optics and Photonics. SPIE, 1999, pp. 22 – 33.

Daniel Wertjanz is doctoral researcher at the Automation and Control Institute (ACIN) at TU Wien, Vienna, Austria. He received an MSc. degree in Electrical Engineering from TU Wien in 2019. His primary research interests are on high performance mechatronic system design, instrumentation, 3D imaging systems, high precision motion control, and robot-based inline measurement systems.

Nikolaus Berlakovich received an MSc degree in Physics from TU Wien in 2016. He is currently pursuing a PhD degree at the Automation and Control Institute (ACIN) of TU Wien. His research interests include registration algorithms and estimation methods related to high-performance optical metrology and precision engineering for automated inline metrology.

Ernst Csencsics is Assistant Professor for Measurement Systems at the Automation and Control Institute (ACIN) of TU Wien. He received an MSc. and a PhD degree (sub auspiciis) in Electrical Engineering from TU Wien, Austria in 2014 and 2017, respectively. His primary research interests are on high performance mechatronic systems, the development of holistic methods for multidisciplinary system design and integration, opto-mechatronic measurement and imaging systems, precision engineering, and advanced robot-based inline measurement systems. He received the journal Best Paper Award of IEEE/ASME Transactions on Mechatronics (2018), the Best Paper Award at the IEEE International Instrumentation and Measurement Technology Conference (2022) and the Best Student Paper Award at the American Control Conference (2016).

Post-print version of the article: D. Wertjanz, N. Berlakovich, E. Csencsics, and G. Schitter, "Range extension for large-scale robotic precision 3D measurements in vibration-prone environments," *IEEE Transactions on Instrumentation and Measurement*,Early Access Version, 2022. DOI: 10.1109/TIM.2023.3268473

Georg Schitter is Professor for Advanced Mechatronic Systems at the Automation and Control Institute (ACIN) of TU Wien. He received an MSc. in Electrical Engineering from TU Graz, Austria (2000) and an MSc. and PhD degree from ETH Zurich, Switzerland (2004). His primary research interests are on high-performance mechatronic systems, particularly for applications in the high-tech industry, scientific instrumentation, and mechatronic imaging systems, such as AFM, scanning laser and LIDAR systems, telescope systems, adaptive optics, and lithography systems for semiconductor industry. He received the journal best paper award of IEEE/ASME Transactions on Mechatronics (2018), of the IFAC Mechatronics (2008-2010), of the Asian Journal of Control (2004-2005), and the 2013 IFAC Mechatronics Young Researcher Award. He served as an Associate Editor for IFAC Mechatronics, Control Engineering Practice, and for the IEEE Transactions on Mechatronics.

Post-print version of the article: D. Wertjanz, N. Berlakovich, E. Csencsics, and G. Schitter, "Range extension for large-scale robotic precision 3D measurements in vibration-prone environments," *IEEE Transactions on Instrumentation and Measurement*,Early Access Version, 2022. DOI: 10.1109/TIM.2023.3268473